AIAA AVIATION Forum
17-21 June 2019, Dallas, Texas
AIAA Aviation 2019 Forum

10.2514/6.2019-3150


# Luminescent Measurement Technique for Analysis of Static and Dynamic Pressure and Strain Fields

Kyle Chism*, Jack Kawell†, James P. Hubner‡
*The University of Alabama, Tuscaloosa, AL 35487-0280*

**Optical techniques such as luminescent coatings sensitive to pressure, temperature, or strain allow for full-field surface measurements in aerodynamic environments. This paper presents the combination of two full-field measurement techniques—pressure sensitive paints and photoelastic coatings—for static and, potentially, dynamic measurement of pressure and strain. Theory, instrumentation, results and issues are discussed.**



## Nomenclature

| | | |
|---|---|---|
| $a$ | = | coating absorptivity |
| $A, B$ | = | PSP calibration coefficients |
| $F, G$ | = | amplitude and phase of the optical strain response |
| $h$ | = | coating thickness |
| $I$ | = | intensity |
| $I'$ | = | relative intensity |
| $K$ | = | photoelastic coating sensitivity |
| $P$ | = | pressure |
| $S_i$ | = | Stokes parameters |
| $\alpha$ | = | analyzer angle |
| $\gamma$ | = | maximum in-plane shear strain |
| $\varepsilon_i$ | = | principal strains |
| $\eta$ | = | coating characteristic |
| $\theta$ | = | principle strain direction |
| $\nu$ | = | Poisson ratio |
| $\lambda$ | = | wavelength |
| $\sigma$ | = | standard deviation |
| $\phi$ | = | polarization efficiency |

| | | |
|---|---|---|
| DL | = | dual-layer |
| DLP | = | degree of linear polarization |
| HPF | = | high-pass filter |
| LED | = | light-emitting diode |
| LP | = | linear polarizer |
| LPC | = | luminescent photoelastic coating |
| OSR | = | optical strain response |
| PEC | = | photoelastic coating |
| PSP | = | pressure-sensitive paint |
| QWP | = | quarter-wave plate |

* Graduate Student, Department of Aerospace Engineering and Mechanics, AIAA Student Member
† Graduate Student, Department of Computer Science at CU-Boulder, NSF REU 2017 summer intern at UA
‡ Associate Professor, Department of Aerospace Engineering and Mechanics, AIAA Associate Fellow

## 1. Introduction

Validation of unsteady theoretical and computational fluid-structure interaction models for flight technologies and systems, particularly pressure fluctuations, requires high temporal and spatial resolution data and corresponding measurement techniques. Acquisition of this data is often compromised by traditional surface and off-surface probes that can interfere and distort the airflow, necessitating substantial correction techniques. Pointwise techniques such as pressure taps, accelerometers and strain gauges, while highly accurate, can have insufficient spatial resolution or add significant time and cost to instrument the model.

This paper introduces an effort to integrate two full-field, optical sensor techniques to measure the unsteady, distributed loads (pressure) and strains on aerodynamically-induced vibrating surfaces and eventually extend into high-speed flows. The approach is to combine fast-response pressure sensitive paints with thin photoelastic coatings to create a fast luminescent pressure and strain measurement technique. The average emission intensity, $I_{avg}$, and amplitude intensity, $I_{amp}$, for a set of pixels sensitive to polarization (Fig. 1) is hypothesized to be sensitive to the pressure, $P$, and maximum in-plane shear strain, $\gamma$, respectively.

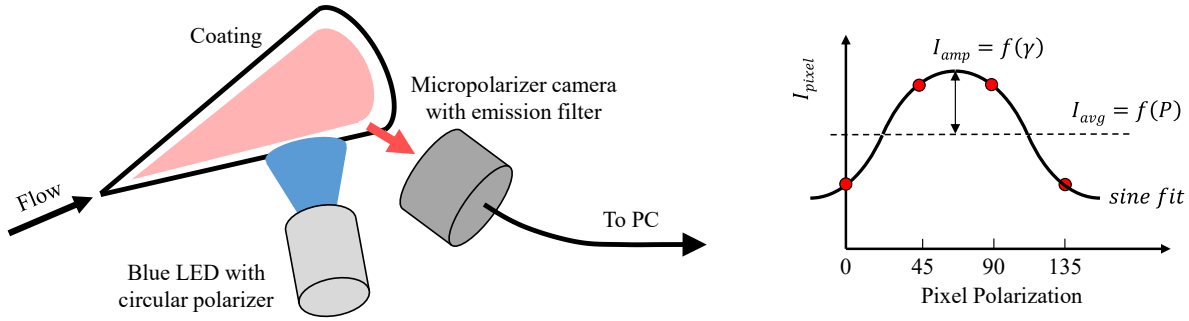


**Figure 1.** Schematic of fast pressure and strain measurement system: each camera superpixel is sensitive to one of four polarization states. Average and amplitude intensity is hypothesized to be sensitive to pressure, $P$, and strain, $\gamma$, respectively.

## 2. Background and Theory

### 2.1 *Pressure Sensitive Paints*

The pressure sensitive paint technique (PSP)[1] has become a common measurement technique in the aerodynamic community and successful implementation of fast pressure sensitive paints (Fast-PSP) have followed due to improvements in paint formulations, ultra-bright light-emitting diodes (LEDs) and high-quantum-efficiency, high-speed digital cameras. A typical PSP is composed of two parts: an oxygen-sensitive fluorescent molecule and an oxygen permeable binder. When a luminescent molecule absorbs a photon, it transitions to an excited energy state. The molecule then typically recovers to the ground state by the emission of a longer-wavelength photon (loss of energy due to thermal relaxation). In some materials, oxygen can interact with the molecule such that the transition to the ground state is non-radiative; this process is known as oxygen quenching. The rate at which these two processes compete is dependent on the partial pressure of oxygen, with a higher oxygen pressure increasing the quenching of the molecule and decreasing the measured luminescence.

Image-based pressure measurements using PSP are accomplished by coating the model surface with the paint and illuminating the surface with light of the appropriate wavelength (usually in the UV to blue range) to excite the luminescent molecules within the coating. The surface is imaged through a bandpass or high-pass filter (HPF) to separate the luminescent signal from the excitation light. The luminescent signal from the paint is not only a function of pressure but also varies with illumination intensity, probe concentration, paint layer thickness, and detector sensitivity. These spatial variations result in a non-uniform intensity map from the painted surface. The spatial variations are usually eliminated by taking the ratio of the luminescent intensity of the paint at an unknown test

condition, $I$, and the luminescent intensity of the paint at a known reference condition, $I_{ref}$. Most PSPs are modeled following the linear Stern-Volmer relationship[1] as shown in Eq. 1

$$\frac{I_{ref}}{I} = A + B\frac{P}{P_{ref}}, \tag{1}$$

a second order polynomial with a third term, $C\left(\frac{P}{P_{ref}}\right)^2$, or a nonlinear dual-sorption model. For Eq. 1, $A$ and $B$ are temperature dependent coefficients and $P$ is pressure.

Conventional PSP formulations typically use a polymer as a binder material. Polymer binders enable the diffusion of oxygen to the embedded dye molecules. The response time of the paint to pressure is largely governed by the rate of oxygen diffusion into the binder which is proportional to the thickness squared and inversely proportional to the binder diffusivity. Thick, conventional formulations have response times on the order of a second. Decreasing the coating thickness to improve response time has the disadvantage of sacrificing luminescent output and signal-to-noise ratio. Porous PSPs use highly porous binders, enhancing the oxygen diffusion and improving the temporal response characteristics. The drawback of a porous PSP is nearly complete quenching at low pressures. Hybrid paint formulations use ceramic particles in the paint, creating a porous structure that decreases the effective thickness, increases the effective diffusivity and extends the pressure range. This results in a fast-response system with favorable signal-to-noise ratio. Hybrid PSP formulations are capable of detecting pressure fluctuations up to $20\,kHz$, and unsteady pressure measurements have been demonstrated on a variety of models[2-5]. Fast-PSP has also been paired with stereo-photogrammetry techniques to measure pressure and deformation[6].

### 2.2 *Photoelastic Coatings*

Photoelastic coatings[7] (PEC) have been used in the structural testing community for many years, primarily for static testing but applicable to dynamic testing related to stress wave propagation and impact[8]. The dynamic response of photoelastic coatings is high due to the propagation of wave speeds through the thin coatings. Typical PEC density and elastic modulus are approximately $1000\,kg/m^3$ and $1\,GPa$, respectively. For a $1\,mm$ thick coating, the theoretical response time based on wave propagation would be approximately$1\,\mu s$.

Photoelastic coatings work on the principle of birefringence: the ability of a material to transmit light at different velocities relative to the polarization and propagation of the incoming light. In application, a reflective photoelastic coating is adhered to the surface of the object (model) of interest and illuminated with circular polarized light (a combination of a linear polarizer and achromatic quarter-wave plate rotated 45° relative to the polarizer). The stress induced change in the polarization as light passes into and reflects out of the coating is measured using an analyzer, a second linear polarizer[§], and a camera. As with all birefringent coatings, the change in polarization is related to the maximum shear strain, $\gamma$, of the specimen. To quantify the strain field, a sequence of images at different analyzer angles is necessary. The development of micropolarizer masks attached to the imager chip eliminates the need of an exterior rotating analyzer and allows multiple analyzer states, typically four, to be acquired with each image. This is an important advancement for dynamic applications.

The luminescent photoelastic coating (LPC) technique[10-11] consists of a luminescent dye in, on or underneath a photoelastic binder. The luminescence creates a more uniform emission field at oblique incidence compared to the reflected field of traditional reflective photoelastic coatings. This higher relative signal on oblique surfaces enables the potential of principal strain separation[12]. The coating luminescence must partially retain the polarization of the excitation to be able to detect the strain-induced birefringence. An absorption dye can be used within the binder—at the expense of lower emission intensity—to limit the excitation penetration depth. Assuming a sufficiently (optically) thick coating, the thickness dependency can be eliminated with the absorption dye. If the coating can be applied with a uniform thickness (sheet application), then the absorption dye is not necessary, increasing the intensity of the detected luminescence of the coating and making it more suitable for shorter exposure times.

The emission intensity of an LPC after it passes through the analyzer is characterized by[10]:

(2)

§ This configuration is sometimes referred to a greyscale polariscope[9]. A more traditional configuration combines a quarter-wave plate and polarizer in front of the imager[7].

$$\frac{I}{I_{avg}} = 1 + F\sin(2\alpha - 2G)$$

where $I$ is the emission intensity at a pixel (or subset of pixels) for a specific analyzer (or micropolarizer) orientation, $I_{avg}$ is the average measured emission intensity over 180° analyzer rotation, $\alpha$ is the analyzer (or micropolarizer) angle, $F$ is the magnitude of the optical strain response (OSR, shown as $I_{amp}$ in Fig. 1) and $G$ is the phase of the OSR. The phase is related to the principal direction of the strain relative to the 0° analyzer angle. The OSR is a function of the in-plane maximum shear strain, $\gamma$. For a single-layer luminescent photoelastic coating with both the luminescent and absorption dyes mixed into the binder, the OSR is[10]

$$F = \phi\frac{\gamma/\eta}{1 + (\gamma/\eta)^2}, \qquad \eta = \frac{a\lambda^*}{2\pi K} \tag{3}$$

where $\phi$ is the polarization-retention efficiency of the luminescence and $\eta$ is the coating characteristic which is a function of the absorptivity, $a$, the coating optical sensitivity, $K$, and the effective excitation-emission wavelength, $\lambda^*$:

$$\lambda^* = \frac{\lambda_{ex}\lambda_{em}}{\lambda_{ex} + \lambda_{em}} \tag{4}$$

The polarization efficiency depends on the ability of the luminescent process to retain the state of excitation polarization after emission. The optical sensitivity is a material property of the coating. If there is no absorption dye in the coating, the luminescent intensity increases and the OSR is[13]

$$F = \phi\frac{1 - \cos(\gamma/\eta)}{\gamma/\eta}, \qquad \eta = \frac{\lambda^*}{2\pi hK} \tag{5}$$

where $h$ is the thickness of the coating. An ideal dual-layer (DL) coating places the luminescent dye above the PEC ($\lambda^* = \lambda_{em}/2$) or below the PEC ($\lambda^* =$ Eq. 4). For these two cases, the polarized emission intensity is

$$F = \phi\sin\left(\frac{\gamma}{\eta}\right), \qquad \eta = \frac{\lambda^*}{2\pi hK} \tag{6}$$

Figure 2 compares theoretical OSR for the coating with an absorption dye, without absorption dye and with the luminescent dye above the coating for $\phi = 1$. The polarization efficiency and coating characteristic are determined through *in situ* or *a priori* calibration. While the latter is easier to implement if known, the former is more accurate, assisting in the elimination of systematic errors that can arise from batch variance, surface reflectance, optical interference and environmental dependencies. The polarization efficiency will be less than one, and the retention of polarization during luminescence depends on the type of luminophor and its concentration.

The coating characteristic, $\eta$, can be thought of as a characteristic strain value that affects the curvature and sensitivity of the OSR amplitude. A larger coating characteristic decreases the OSR sensitivity but extends its range to the first peak location. This is important to reduce the difficulty in determining a unique solution. For values of $\gamma/\eta$

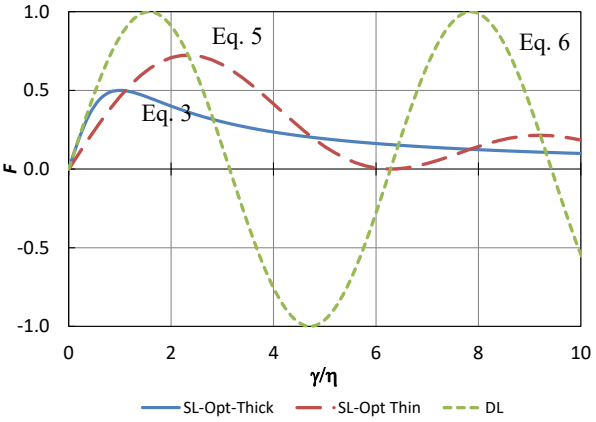


**Figure 2.** Optical strain response, $F$, of a single-layer coating with absorption dye (blue solid line, Eq. 3), single-layer coating without absorption dye (red dash line, Eq. 5), and dual-layer coating (green dotted line, Eq. 6)

beyond the first OSR peak, the relationship is multi-valued requiring fringe counting and phase-unwrapping techniques. There are multiple approaches to extend OSR range: decrease the coating thickness, use a PEC with lower optical sensitivity, $K$, or increase the effective wavelength. The latter approach depends on the absorption and emission properties of the luminescent coating.

### 2.3 *Combined Technique*

The combined technique, a dual-layer coating (Eq. 6), uses a PSP sprayed on top of a photoelastic coating, enabling oxygen quenching of the PSP and creating a luminescent pressure and strain sensitive coating. Figure 3 is a schematic of the excitation and emission of the concept. The coating is excited with circular-polarized light in the absorption bands of the luminescent probe ($\lambda_{ex}$ ~ ultraviolet to blue). The corresponding luminescence is Lambertian (diffuse) in nature. If the PSP is not optically thick, then part of the emission detected by the camera will have doubly passed through the coating, reflecting off the surface. If the PSP emission partially retains the circular polarization, then the stressed-induced birefringence of the PEC undercoat will modify the emission polarization. A high-pass (or bandpass) optical filter is necessary to block the excitation and allow the polarized emission to pass through to the imager. If the emission is captured through a pixelated polarizer mounted on the imaging sensor, then each pixel will measure an intensity relative to the polarization orientation of that pixel. A typical micropolarizer array has four discrete orientations in a $2 \times 2$ pattern: $0/45/90/135°$. The group of four pixels is called a superpixel.

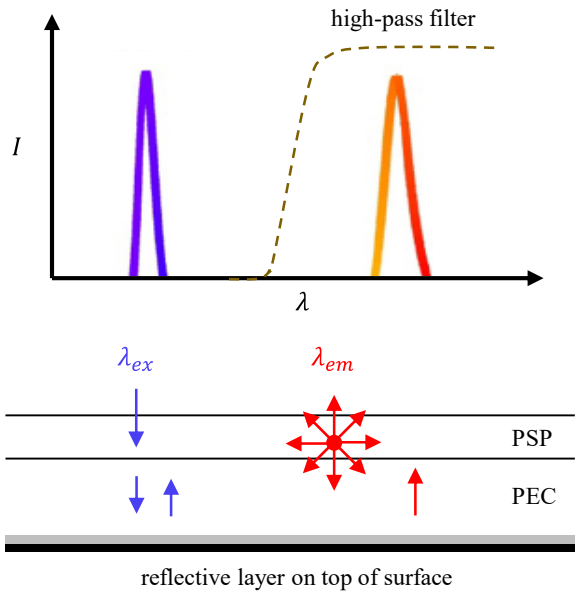


**Figure 3.** Emission paths for the overlay paint approach

While the emission intensity recorded by each pixel is dependent on strain, pressure, excitation intensity and coating thickness/concentration, the dual coating response is modeled assuming the strain information is carried in the polarization of the emission and the pressure information is carried in the average intensity of the emission. As such, the average of a superpixel is strain independent based on the sinusoidal form of Eq. 2—assuming an even number of analyzer angles appropriately oriented. For a superpixel,

$$I_{avg} = \bar{I} = \frac{(I_0 + I_{45} + I_{90} + I_{135})}{4} \neq f(\gamma) \tag{7}$$

In terms of the pressure response, $I_{avg}$ is the effective superpixel intensity, thus

$$\frac{\overline{I_{ref}}}{\bar{I}} = A + B\frac{P}{P_{ref}}, \tag{8}$$

Substituting Eq. 8 into Eq. 2 for a dual-layer coating yields,

$$\frac{I}{\overline{I_{ref}}} = \frac{1}{A + B\dfrac{P}{P_{ref}}}\left(1 + \phi\sin\left(\frac{\gamma}{\eta}\right)\sin(2\alpha - 2G)\right) \tag{9}$$

where $\overline{I_{ref}}$ is the unloaded, reference pressure state for a superpixel. Eq. 9 is a sinusoid function with a relative intensity amplitude and intensity offset equal to

$$I'_{amp} = \frac{\phi \sin\left(\frac{\gamma}{\eta}\right)}{A + B\frac{P}{P_{ref}}} \qquad \text{and} \qquad \overline{I'} = \left(\frac{\bar{I}}{\overline{I_{ref}}}\right) = \frac{1}{A + B\frac{P}{P_{ref}}} \qquad (10a\text{-}b)$$

respectively. Theoretically, each superpixel represents a pressure and strain state on the surface of the model at that pixel. Image processing techniques like pixel binning, image registration and spatial filtering can be used to improve signal-to-noise ratio.

The relative intensity amplitude, $I'_{amp}$, contains both pressure and strain information. Dividing by $\overline{I'}$ yields the OSR magnitude, $F$. To determine $I'_{amp}$ or $F$, Eq. 9 or Eq. 2, respectively, is fit with a sine function relative to $\alpha$. A non-linear fit algorithm such as the Levenberg-Marquart routine is suitable and also yields the phase, $2G$, which is related to the principal strain direction. Alternatively, and more computationally efficient, the standard deviation of $\frac{I}{\overline{I_{ref}}}$ for a superpixel can be used to calculate the relative amplitude,

$$I'_{amp} = \frac{\sigma_I}{\overline{I_{ref}}} \qquad (11)$$

where $\sigma_I$ is the standard deviation of the four polarization intensities relative to $1/\sqrt{N}$. In cases where the strain is zero or at a fringe node, the intensity ratio is constant with respect to analyzer orientation and $I'_{amp} = 0$. If the relative amplitude is not zero at the reference state (e.g., residual birefringence in the coating), then a vector subtraction of the residual state is necessary[14,15]. Finally, relative amplitude is a sinusoidal function of the maximum shear strain; thus, multiple values of $\gamma$ can exist for a single value $I'_{amp}$ if the coating characteristic, $\eta$, is too small (Section 2.2). By using a coating thickness such that $\frac{\gamma_{max}}{\eta} < \frac{\pi}{2}$ or $\gamma_{max} < \frac{\lambda^*}{4hK}$, then the need for fringe counting or phase-unwrapping is eliminated assuming a negligible OSR amplitude at the reference state.

## 3. Test Apparatus

Figure 4 is a schematic of the test apparatus. The excitation source is an air-cooled ISSI LM3X 405 nm LED lamp. This lamp uses three 12 $W$ LEDs. Aligned in the LED excitation path is a linear polarizer and an achromatic QWP, rotated at 45° relative to the polarizer, to create circular polarized light. The pair of 50 $mm$ diameter optics is placed approximately 10 $cm$ in front of the LED to alleviate heating and damage of the polarizer. The imager is a 4D-Technologies PolarCam U2 CMOS camera with a 0/45/90/135° linear polarization mask for each superpixel. The maximum full-field frame rate is 164 $fps$ at 12-bit. Attached to the camera is a Nikon 50 $mm$ lens set at an $f$-stop of 1.2. A 570 $nm$ HPF is attached to the lens when measuring emission intensities.

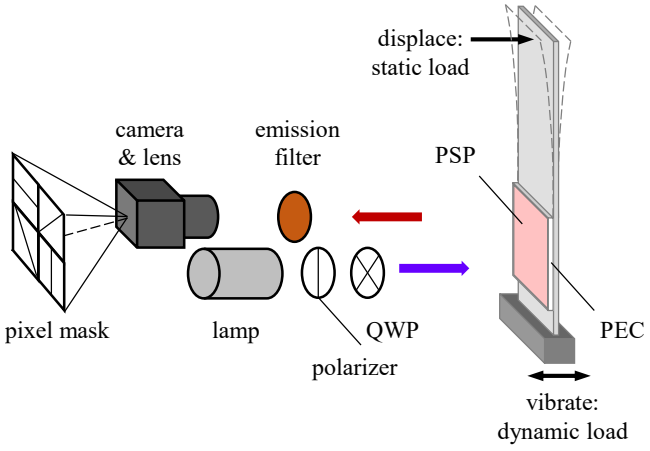


**Figure 4.** Emission paths for the overlay paint approach

The specimens are thin aluminum (6061-T6) cantilever beams. A custom-built pressure and shake chamber, Fig. 5, can accommodate specimens 1 – 3 $mm$ thick, 20 – 30 $mm$ wide and < 250 mm long. For this test, the specimens were 1.6 $mm$ × 25 $mm$ × 250 $mm$. The chamber is capable of controlling the pressure between 10 $kPa$ to

$101\ kPa$. The beams are clamped at one end and either statically loaded via a displacement screw at the other end or dynamically loaded using a shaker rod passing through the chamber backside and connecting to the beam mount. Based on the thickness and length of the beam, resonance can be controlled, typically in the range of $20-30\ Hz$. Under elastic load conditions, the induced stress in the cantilever specimen will be theoretically linear with the maximum at the clamped base (bottom). PEC thickness will locally reinforce the specimen. The reinforcement depends on the coating thickness, specimen thickness, coating type, base material and type of loading[14]. For this test, the coating-to-specimen thickness ratio is 0.32 and a fringe correction factor of 0.85 was determined. The principal stress aligns along the length of the beam, and the corresponding maximum in-plane shear strain is $\gamma = \varepsilon_1 - \varepsilon_2 = (1+\nu)\varepsilon_1$.

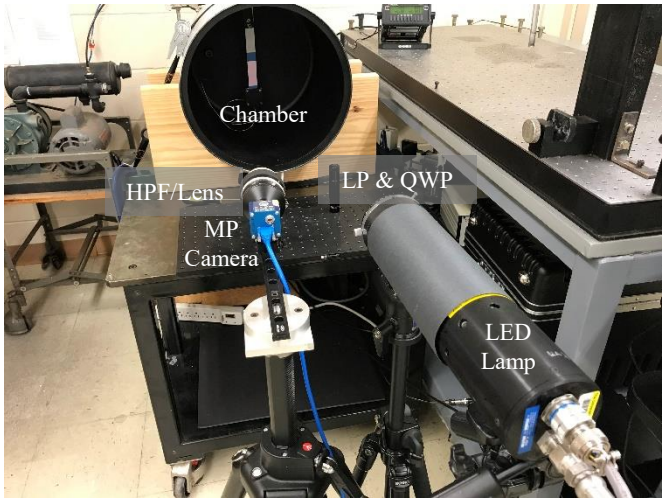


**Figure 5.** PSP-PEC test apparatus

A $75-100\ mm$ strip of PEC (Micro-Measurement's PS-1; $h$ = 0.5 mm & $K$ = 0.15) was adhered with PC-10 reflective adhesive near the clamped end of the specimen. A thin layer of ISSI's PtTFPP-PP Fast-PSP ($A$ = 0.3, $B$ = 0.7)[16] was sprayed on the surface. The center absorption band of the PSP is $400\ nm$, and the center emission band is $650\ nm$. Based on the thickness of the photoelastic coating and the excitation and emission parameters of the Fast-PSP, the coating characteristic is 690 $\mu\varepsilon$[**].

## 4. Results and Discussion

### 4.1 *PSP Polarization Retention*

To test the polarization retention of the coating, the degree of linear polarization was measured (Eq. 12)[17]:

$$DLP = \frac{\sqrt{S_1^2 + S_2^2}}{S_o} \tag{12}$$

where

$$S_o = 2I_{avg}\,, \quad S_1 = I_0 - I_{90}\,, \quad S_2 = I_{45} - I_{135} \tag{13a-c}$$

The value for DLP ranges from 0 (circular or unpolarized) to 1 (linear polarized). While it is expected that the PEC will have high polarization retention, the luminescence of the PSP is expected to be lower. A randomly distributed orientation of the luminophors would have a DLP near 0.5. Losses in the emission process and dependence on the luminophor concentration will lower the polarization retention further.

First, the DLP of the PEC was tested. A linear polarizer was placed in front of the LED lamp, and the LED excitation was directed towards the PEC adhered to the specimen. The reflection of the unstrained PEC was captured with the micropolarizer camera but without the high-pass filter as the PEC does not luminesce. The measured DLP was 0.89, indicating a high retention of polarization as expected. Next, the PSP-PEC coating was tested in a similar

[**] $\mu\varepsilon$ = microstrain or $\mu m/m$

fashion, with the high-pass filter attached to the camera lens to isolate the luminescent emission from the excitation. The measured DLP ranged between 0.06 to 0.12. While low, partial polarization was preserved and the potential for strain detection exists.

### 4.2 *Combined Pressure and Strain Response*

A dual-coated, cantilever specimen was first tested to assess the pressure response. The specimen was placed in the test chamber, and the pressure was lowered from 101 $kPa$ to 32 $kPa$ ($P/P\_ref$ = 1.00 to 0.32) with no applied stress to the specimen. All images were post-processed with a 9 × 9 mean smoothing filter. Figure 6 shows full-field, false-color $\overline{I_{ref}}/\bar{I}$ surface response of the superpixels where $\overline{I_{ref}}$ is the atmospheric pressure image. As the pressure is lowered (left to right), the emission intensity increases and the corresponding intensity ratio decreases (red to blue). Figure 7 shows the response with an applied stress ($\gamma_{base} = 800\ \mu\varepsilon$). The results match Fig. 6, indicating strain independence of the $I_{avg}$ signal. To note, image registration was not performed and likely accounts for some of the spatial variance in the processed images, particularly at the edges of the specimen.



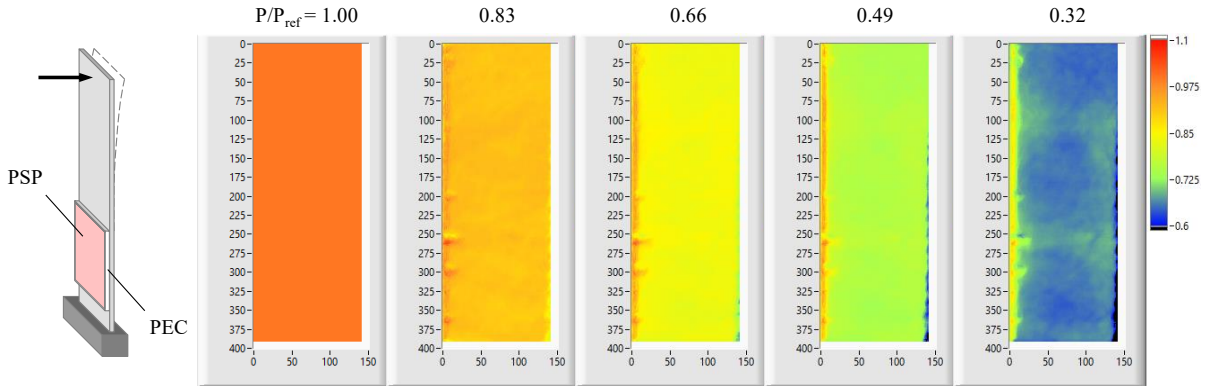


**Figure 6.** Full-field, false-color $\overline{I_{ref}}/\bar{I}$ response of the PSP-PEC coating to pressure and no applied strain: $\gamma_{base} = 0\ \mu\varepsilon$, numbers on axes indicate pixel location

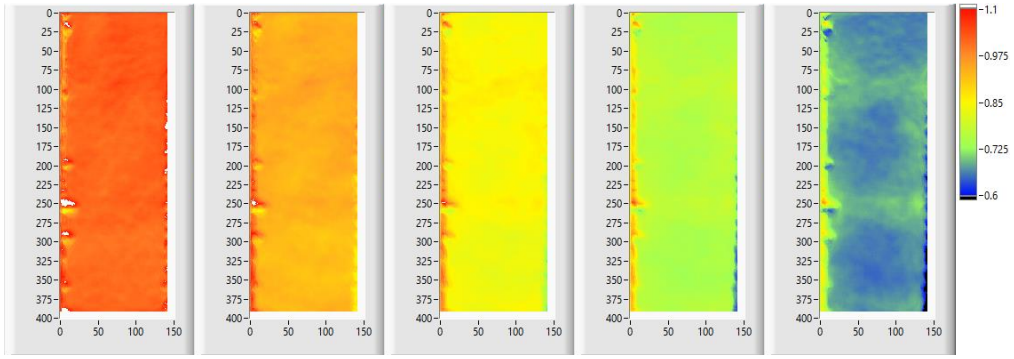

**Figure 7.** Full-field, false-color $\overline{I_{ref}}/\bar{I}$ response of the PSP-PEC coating to pressure and with applied strain: $\gamma_{base} = 800\ \mu\varepsilon$

Figure 8 plots the Stern-Volmer curve for the PSP-PEC coating at a pixel near the center of the specimen. For the two load cases, the measured pressure sensitivity is the same, again indicating strain independence. However, the slope, $B = 0.5$, is not as high as expected for the PSP[16] and indicates an outside interference likely related to the filtering of the emission.

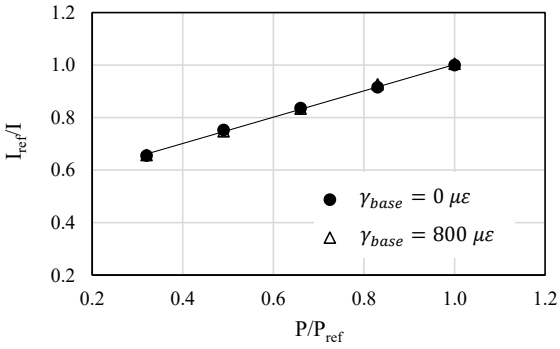


**Figure 8.** $\overline{I_{ref}}/\bar{I}$ pressure response for a superpixel:

Figure 9 shows the intensity ratio, OSR magnitude and phase for the specimen with a load applied at atmospheric conditions (and no chamber window). The reference state is $P_{ref} = 101\ kPa$ and $\gamma_{ref} = 0\ \mu\varepsilon$. Along the top row of Fig. 9, the intensity ratio is constant indicating the constant pressure acting on the specimen. Minor registration and camera noise are present but small ($< 1\%$).

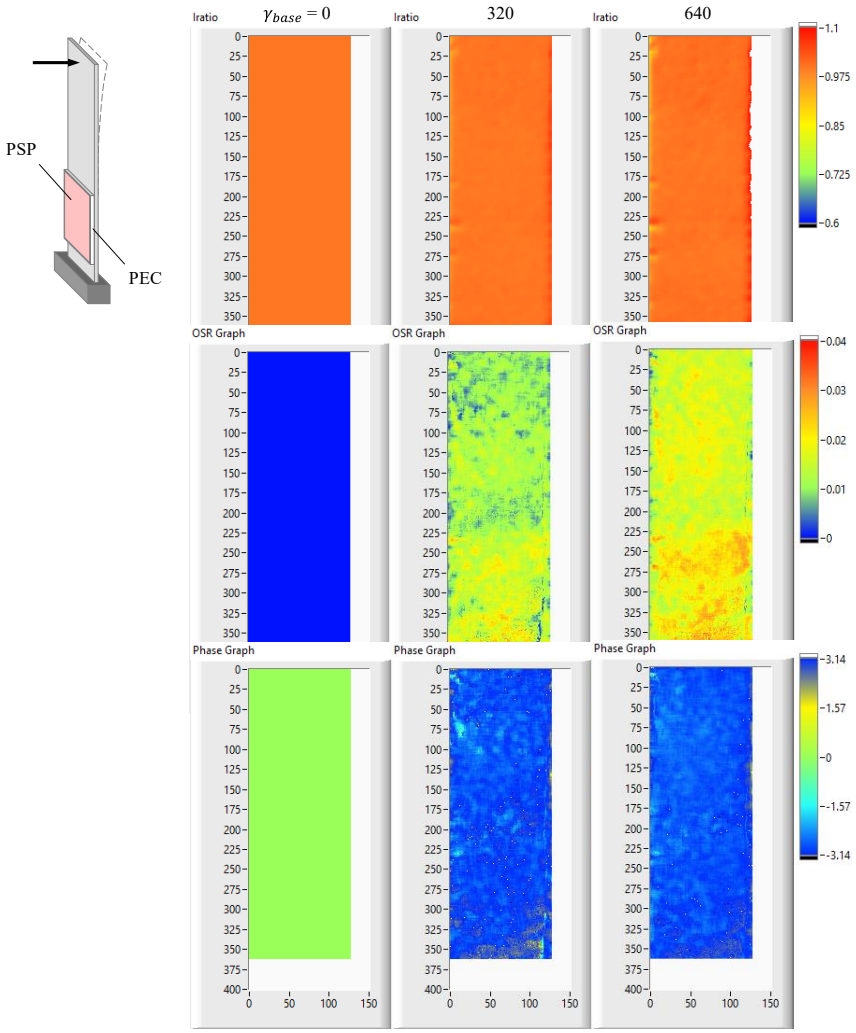


**Figure 9.** Full-field, false-color $\overline{I_{ref}}/\bar{I}$ response of the PSP-PEC coating to applied strain and atmospheric pressure

Along the middle row of Fig. 9, the relative magnitude of the OSR is mapped. While small compared to the sensitivity in pressure, increasing strain increases the OSR magnitude. Images from left to right correspond to higher strain, and the bottom of each image corresponds to higher strain relative to the top of the image. The phase map of the OSR is plotted along the bottom row of Fig. 9. The phase contour indicates the principal strain direction of the strain and is equal to $\theta \approx \pm\pi/2$ (blue) when the load is applied. This is expected as the horizontal polarizer orientation is considered 0° and the maximum principal strain direction for the loaded specimen would be along the length of the cantilever beam or $\theta = 90°$.

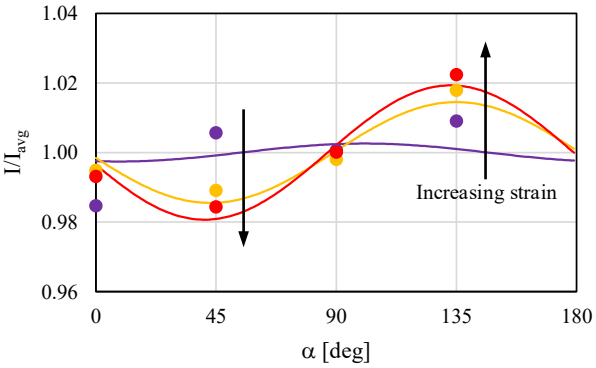


**Figure 10.** The OSR response for a superpixel at atmospheric pressure and increasing strain

To calculate the OSR, a sine fit of the intensity measurements relative to the polarization states of a superpixel was performed for each image (applied pressure and strain state). As discussed in Section 2.3, the standard deviation of the intensities could also be used and requires less computational time for large data sets. An example of the fit for a selected superpixel is shown in Fig. 10. The individual symbols show intensity relative to the superpixel average for each polarization state and test condition (color of symbol). The corresponding sine fit for each test condition is shown as a line plot. At the reference state (purple), a low amplitude response is measured due to either interference (e.g., residual stress in the coating or window) or system noise. A vector subtraction[14,15] of the reference state from the test state is performed to calculate the load-induced OSR magnitude and phase shown in the full-field maps of Fig. 9.

Figure 11 shows the effect of an optical window on the strain response. The four image maps show the reference state OSR magnitude and phase with and without a window on the test chamber. For the case without the window (upper left), the OSR magnitude is smaller and less structured than the case with the window (upper right). Also, the OSR phase without a window (lower left) is less preferentially oriented than with the window (lower right). This is the expected because optical windows are generally birefringent. Ideally, in the reference state, the OSR magnitude would be zero. However, for the case without the window, interference sources such as coating residual stress and elliptically polarized excitation as well as noise sources from the coating and camera can lead to a non-zero reference OSR and non-preferential phase orientation. If small relative to the strain-induced OSR, the reference state OSR can be neglected. For the case with the window, residual stress as well as pressure-induced stress in the window can lead to OSR interference and a preferential phase orientation. Thus characterization of the window response is necessary and is currently being studied.

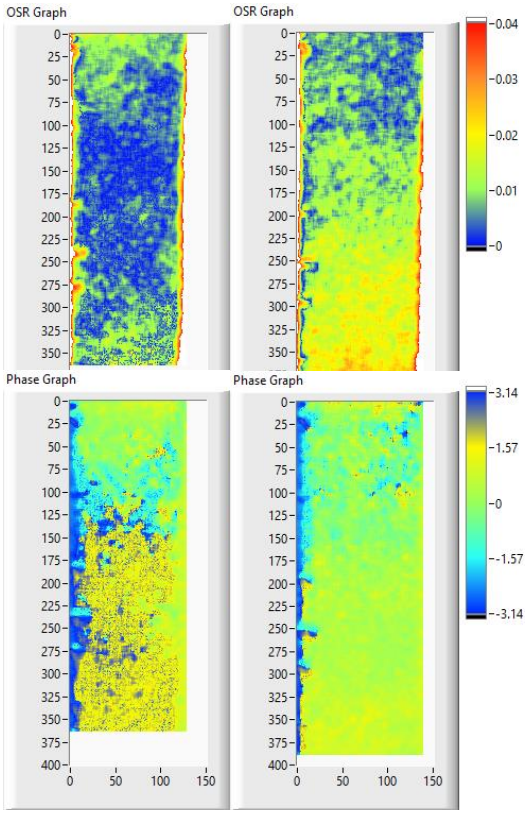


**Figure 11.** Comparison of the reference OSR magnitude and phase without (left) and with (right) window: atmospheric conditions, no applied load

### 4.3 *Towards Dynamic Measurements*

A long term objective of this research is to develop the technique for dynamic applications and transition into wind tunnel testing. As discussed in Section 3, the benchtop test chamber is designed to vibrate the specimens at their resonant frequency to induce large strains near the base of the beam with small displacements of the base. For this configuration, the maximum shear strain will peak twice per oscillation. The corresponding phase will alternate between 0 and $\pi/2$, switching when the coated side of the beam passes from compression to tension. Future research will test PEC-PSP specimens under dynamic loads, focusing on enhancing signal strength and developing processing techniques for larger data sets.

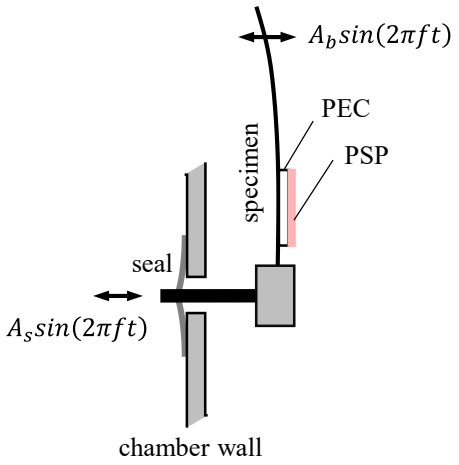


**Figure 12.** Schematic of resonance-induced strain in the specimen: $A_b/A_s > 1$, coating thickness exaggerated

## 5. Conclusions

The theory modeling the response of a dual-layer coating with pressure-sensitive paint on the top and a photoelastic coating underneath is presented. As modeled, the surface pressure and maximum shear strain response are related to the intensity average and standard deviation, respectively, of a superpixel with multiple polarization orientations. Experimental results on a cantilever beam support the predicted response and show that the pressure signal is stronger than the strain signal. Interference due to window birefringence does not appear affect the pressure signal but can affect the strain signal.

## 6. Acknowledgements

This project is supported by NSF and AFOSR Grant CBET-1802994: Dr. R Joslin and Dr. I Levya program managers. The authors would like to thank ISSI and Dr. Jim Crafton for the PSP supplies. Mr. Kawell was supported by an NSF REU site program: EEC 1659710.



## References

1. Liu, T, and JP Sullivan, *Pressure and Temperature Sensitive Paints*, Springer-Verlag, Berlin, 2004.
2. Crafton, J, A Forlines, S Palluconi, KY Hsu, C Carter, and M Gruber, "Investigation of Transverse Jet Injections in a Supersonic Crossflow Using Fast-Responding Pressure-Sensitive Paint," *Experiments in Fluids*, **56**(27), 2015, DOI 10.1007/s00348-014-1877-3.
3. Flaherty, W, TM Reedy, GS Elliott, JM Austin, RF Schmit, and J Crafton, "Investigation of Cavity Flow Using Fast Response Pressure Sensitive Paint", *AIAA Journal*, **52**(11):2462-2470, 2014.
4. Gregory, JW, K Asai, M Kameda, T Liu, and JP Sullivan, "A Review of Pressure-sensitive Paint for High Speed and Unsteady Aerodynamics," *Proceedings of the Institution of Mechanical Engineers, Part G, Journal of Aerospace Engineering*, **222**(2):249-290, 2008.
5. Casper, KM, JL Wagner, SJ Beresh, RW Spillers, and JF Henfling, "Study of Fluid-Structure Interactions on a Tunable Store in Complex Cavity Flow, AIAA Paper 2017-3125, June 2017.
6. Spottswood, SM, TJ Beberniss, and T Eason "Full-Field, Dynamic Pressure and Displacement Measurements of a Panel Excited by Shock Boundary-Layer Interaction," AIAA Paper 2013-2016, May 2013.

7. Zandman, FS, Redner, and JW Dally, *Photoelastic Coatings*, Iowa State University Press, Ames, IA, 1977.
8. Dally, J, "An Introduction to Dynamic Photoelasticity," *Experimental Mechanics*, **20**(12):409-416, 1980.
9. Lesniak, JR, and MJ Zickel, "Applications of Automated Grey-field Polariscope," *Proceedings of Society of Experimental Mechanics*, 298-301, June 1998.
10. Hubner, JP, L Chen, Y Liu, K Schanze, J Nicolosi, P Ifju, and W El-Ratal, "Characterization of a New Luminescent Photoelastic Coating," *Experimental Mechanics*, **45**(2):137-143, 2005, DOI: 10.1007/BF02428186
11. Chen, L, PG Ifju, JP Hubner, and J Nicolosi, "Full-field Strain Analysis of Composite Structures using Luminescent Photoelastic Coatings," ASC/ASTM-D30 Joint 19th Annual Technical Conference, October 2004.
12. Esirgemez, E, and JP Hubner, "Luminescent Photoelastic Coating Image Analysis and Strain Separation on a Three-dimensional Grid," *Optical Engineering*, **49**(8), 2010, DOI: 10.1117/1.3475946.
13. Hua, SQ, and Y Luo, "Improvement of the Coating Formulation in Luminescent Photoelastic Coating Method," *Experimental Techniques*, **37**(4):19-24, 2013.
14. Tech Note TN-706-1, "Corrections to Photoelastic Coating Fringe-Order Measurements," Micro-Measurements, Rayleigh, NC, August 2015.
15. Hubner, JP, and L Chen, "Coupled Strain and Fresnel Response of Photoelastic Coatings at Oblique Incidence," Experimental Mechanics, **47**(4):549-560, 2007, DOI: 10.1007/s11340-007-9033-0.
16. "Porous, Fast Responsive Pressure Sensitive Paint: FP-XXX," Innovative Scientific Solutions, Inc., Dayton, OH, n.d.
17. Zecchino, M, *PolarView™ User Manual*, 4D Technology Corporation, Rev. 2.3.0.0 A, Tucson, AZ, June 2017.